

# Geophysical Research Letters®



## RESEARCH LETTER

10.1029/2025GL120126

## Shifts in the Annual Cycle and Associated Impacts on Northern Hemisphere Summer Onset Under Global Warming

### Key Points:

- Annual cycle changes have delayed summer onset across many midlatitude regions, particularly over North America and Central Asia
- Phase delays mainly result from increased effective heat capacity and reduced damping
- Greenhouse gas forcing advances onset by reducing heat capacity and enhancing damping, whereas aerosols delay onset via opposite effects

Ruyu Gan<sup>1</sup> , Kaiming Hu<sup>2</sup> , Gang Huang<sup>3,4</sup> , Xiaofan Ma<sup>5,6</sup>, and Qi Liu<sup>7</sup> 

<sup>1</sup>Ocean College, Jiangsu University of Science and Technology, Zhenjiang, China, <sup>2</sup>College of Resource Environment and Tourism, Capital Normal University, Beijing, China, <sup>3</sup>Key Laboratory of Earth System Numerical Modeling and Application, Institute of Atmospheric Physics, Chinese Academy of Sciences, Beijing, China, <sup>4</sup>University of Chinese Academy of Sciences, Beijing, China, <sup>5</sup>State Key Laboratory of Climate System Prediction and Risk Management/Key Laboratory of Meteorological Disaster, Ministry of Education/Collaborative Innovation Center on Forecast and Evaluation of Meteorological Disasters/Institute of Climate and Application Research, Nanjing University of Information Science and Technology, Nanjing, China, <sup>6</sup>School of Atmospheric Sciences, Nanjing University of Information Science and Technology, Nanjing, China, <sup>7</sup>School of Atmospheric Sciences, Nanjing University, Nanjing, China

### Supporting Information:

Supporting Information may be found in the online version of this article.

### Correspondence to:

K. Hu and G. Huang,  
[hkm@mail.iap.ac.cn](mailto:hkm@mail.iap.ac.cn);  
[hg@mail.iap.ac.cn](mailto:hg@mail.iap.ac.cn)

### Citation:

Gan, R., Hu, K., Huang, G., Ma, X., & Liu, Q. (2026). Shifts in the annual cycle and associated impacts on Northern Hemisphere summer onset under global warming. *Geophysical Research Letters*, 53, e2025GL120126. <https://doi.org/10.1029/2025GL120126>

Received 17 OCT 2025

Accepted 6 FEB 2026

### Author Contributions:

**Conceptualization:** Ruyu Gan  
**Funding acquisition:** Ruyu Gan, Kaiming Hu, Gang Huang, Xiaofan Ma  
**Investigation:** Ruyu Gan, Kaiming Hu  
**Methodology:** Ruyu Gan  
**Software:** Ruyu Gan  
**Supervision:** Kaiming Hu, Gang Huang  
**Validation:** Ruyu Gan  
**Visualization:** Ruyu Gan  
**Writing – original draft:** Ruyu Gan, Kaiming Hu  
**Writing – review & editing:** Ruyu Gan, Kaiming Hu, Gang Huang, Xiaofan Ma, Qi Liu

**Abstract** Global warming has altered the timing of seasonal onset, yet the relative roles of long-term mean warming and changes in the annual cycle (AC) remain unclear. Using observational data sets and CMIP6 simulations, here we quantify how long-term warming and the AC contribute to changes in seasonal onset across Northern Hemisphere midlatitudes during 1950–2014. While long-term warming drives a widespread advance of summer onset, regional, and latitudinal contrasts arise primarily from AC variations. In North America and northern Asia, these cycle changes offset the warming-induced advance and contribute at magnitudes comparable to long-term warming, highlighting their critical role in shaping regional climate responses. Based on single-forcing experiments and a simplified surface energy balance model, we further show that greenhouse gases enhance damping and reduce effective heat capacity, advancing the AC phase, whereas aerosol forcing increases effective heat capacity and weakens damping, thereby delaying summer onset.

**Plain Language Summary** Climate change is making summers start earlier, but natural seasonal cycles can delay this shift in some regions. Using climate models, we found that while long-term warming pushes summers to arrive sooner overall, the phase changes in the annual cycle (AC) slow this effect in regions such as North America and North Asia. Aerosols and greenhouse gases also change these natural cycles, creating stronger regional differences. In many areas, AC influences summer timing as much as long-term warming does. We also show how basic atmospheric processes help explain why greenhouse gases and aerosols affect seasons differently.

## 1. Introduction

The seasonal cycle constitutes a primary mode of natural variability within the atmospheric system, exerting profound influences on biological rhythms (Cleland et al., 2007; Horton et al., 2020), agricultural productivity (Matiu et al., 2017; T. Park et al., 2016), and human health (Ryan et al., 2019). Many studies have demonstrated that plant phenology (Buermann et al., 2018; Reyes-Fox et al., 2014; Steltzer & Post, 2009) and bird migration (Both et al., 2006; Horton et al., 2020) are highly sensitive to changes in the timing and structure of the seasonal cycle. For instance, an earlier spring onset across the midlatitudes has been associated with longer growing seasons, with implications for ecosystem dynamics (M. D. Schwartz et al., 2006), and carbon cycling (Keeling et al., 1996) as well as allergenic pollen exposure (Anenberg et al., 2017).

The dominant manifestation of the seasonal cycle varies across climate regimes. In the tropics, it is expressed primarily through the annual cycle (AC) of precipitation (Lv et al., 2024; F. Song et al., 2020, 2023). Over the midlatitudes, the temperature seasonal cycle is more pronounced and plays a central role in shaping both ecological responses and large-scale atmospheric processes. For example, the modulation of the temperature seasonal cycle can have far-reaching climatic impacts, influencing atmospheric eddy activity, storm tracks, and heatwave frequency (García-Herrera et al., 2010). Given its wide-ranging implications, much attention has

© 2026. The Author(s).

This is an open access article under the terms of the [Creative Commons Attribution License](https://creativecommons.org/licenses/by/4.0/), which permits use, distribution and reproduction in any medium, provided the original work is properly cited.

focused on the characteristics, variability, and long-term changes in seasonal cycle (Duan et al., 2019; Jo et al., 2022; Liu et al., 2024; Santer et al., 2018, 2022; Shi et al., 2024; Yang et al., 2025).

Under ongoing global warming, both the phase and amplitude of the temperature seasonal cycle have experienced pronounced changes. Previous studies have documented the advancement of spring and summer onsets (Donohoe et al., 2020; Paluš et al., 2005; Peña-Ortiz et al., 2015; Sparks & Menzel, 2002; Stine et al., 2009) and the delay of autumn and winter onsets across various regions (Christidis et al., 2007; Menzel, 2000). Multimodel attribution studies identify greenhouse gas (GHG) warming as the dominant driver of these changes (Lin & Wang, 2023; B.-J. Park et al., 2018; J. Wang et al., 2021). Consistently, single-forcing simulations from the Coupled Model Intercomparison Project Phase 5 (CMIP5) and Phase 6 (CMIP6) attribute the lengthening of boreal summer and earlier summer onset in the Northern Hemisphere (NH) primarily to GHG-induced warming (B.-J. Park et al., 2018; J. Wang et al., 2021).

At the same time, emerging evidence suggests that changes in the structure of the seasonal temperature cycle may also influence seasonal onset. Variations in the phase and amplitude of the AC are increasingly documented (Chiang et al., 2022; Dwyer et al., 2012; Liu et al., 2020; Qian & Zhang, 2015; Timmermann et al., 2004; Wu et al., 2008; Yang & Wu, 2024) and are regarded as critical factors influencing changes in the timing of seasonal onset (Menzel, 2000). For example, Qian et al. (2011) showed that shifts in the phase of the AC account for approximately 40%–60% of the observed trend in spring onset in northeastern China. Moreover, Deng et al. (2023) decomposed near-surface temperature into a long-term trend, the AC, and the semiannual cycle (SAC), and demonstrated that the AC and SAC components can exert opposing influences on seasonal onset over China. These results imply that changes in the structure of the temperature seasonal cycle may modulate seasonal transitions. However, existing evidence remains largely confined to regional scales, and the broader hemispheric relevance of this mechanism has not yet been assessed.

These results indicate that observed shifts in seasonal onset may arise from both long-term mean warming and changes in the structure of the seasonal cycle. Although long-term mean warming and changes in the AC are both recognized as important contributors, their respective roles have not been quantitatively separated, and the influence of anthropogenic forcing on each component remains poorly understood. Here we quantify the relative contributions of long-term warming and the AC to summer onset changes across NH midlatitudes during 1950–2014. Using observational data sets and CMIP6 DAMIP single-forcing simulations, we demonstrate how GHGs and aerosols exert opposing influences on AC, shaping regional contrasts in summer onset. Based on a simplified surface energy balance model, we show how variations in atmospheric damping and thermal inertia explain the differing seasonal responses to GHGs and aerosols. Our findings highlight that changes in the AC, acting as an indirect response to anthropogenic warming, can partially offset the effects of long-term mean warming, reshaping regional patterns of seasonal onset.

## 2. Materials and Methods

### 2.1. Observations, Reanalysis Data, and CMIP6 Data

Our analysis uses daily mean temperature from two data sets: Berkeley Earth Surface Temperature (BEST) for 1880–2022 (Rohde & Hausfather, 2020) and ERA5 (1950–2024, Hersbach et al., 2020), with a focus on the years 1950–2014. Results primarily use Berkeley data, with other data sets shown in Figures S3 and S4 in Supporting Information S1. Using nine CMIP6 models (Gillett et al., 2016), we examine the role of external forcings in seasonal-onset changes. Historical simulations include combined natural and anthropogenic forcings, while hist-nat, hist-GHG, and hist-aer simulations isolate natural, GHG, and aerosol (AER) effects. Model details are in Table S1 in Supporting Information S1.

### 2.2. Definitions of Season Onsets

Following previous studies (Christidis et al., 2007; B.-J. Park et al., 2018; J. Wang et al., 2021), we define the onset of the four seasons using local temperature thresholds. At each grid point, we smooth daily temperature with a fifth-degree polynomial fit to suppress day-to-day variability and identify onset dates (Deng et al., 2023; B.-J. Park et al., 2018; J. Wang et al., 2021). Robustness is assessed using a seventh-degree fit (Figures S11 and S12 in Supporting Information S1).

We define seasons using temperature thresholds: summer starts when daily temperatures exceed the 75th percentile (1950–2014 average), and winter begins when they drop below the 25th percentile. Autumn starts when temperatures first fall below the 75th percentile after summer, while spring begins when they rise above the 25th percentile after winter. 29 February is excluded. This study focuses on summer, with autumn/winter/spring results in Supporting Information S1.

### 2.3. Definition of Contributions From Annual Cycle and Long-Term Trend to Season Onsets

We decomposed each year's smoothed daily temperature curve based on the fifth-degree polynomial fitting into five additive components: the AC, the SAC, a constant baseline (CB), a long-term trend (LTC), and interannual variability (IAV). This framework provides a physically interpretable decomposition of seasonal temperature evolution.

The AC and SAC components were extracted by applying a Fourier transform to each year's smoothed seasonal cycle, isolating the annual and semiannual harmonics following Stine et al. (2009):

$$a = \frac{1}{365} \sum_1^{365} e^{\frac{2\pi i k n}{365}} x'(n) \quad (1)$$

where  $x'(n)$  is the smoothed temperature at day  $n$ , and  $k = 1$  and  $2$  correspond to the AC and SAC, respectively. The associated harmonic component is:

$$Y_k(n) = 2\text{Re}\left(ae^{-\frac{2\pi i k n}{365}}\right) \quad (2)$$

Accordingly, the AC and SAC are defined as  $Y_1(n)$  and  $Y_2(n)$ , respectively.

Since the annual averages of AC and SAC are zero, we further decomposed the annual averages of the smoothed daily temperature curve for each year (1950–2014) into: (a) CB: 1950 baseline temperature, (b) LTC: the linear warming trend, and (c) IAV: residual IAV. The complete reconstruction is: AC + SAC + CB + LTC + IAV. Figure S6 in Supporting Information S1 confirms this decomposition accurately reproduces the seasonal cycle, with IAV having minimal impact on long-term trends.

To isolate the influence of each component, we constructed four composite series: (a) AC + CB, (b) AC + CB + SAC, (c) AC + CB + LTC, and (d) AC + CB + IAV. For each composite, we calculated 1950–2014 linear trends in seasonal onset dates. Differences relative to AC + CB quantify the contributions of SAC, LTC, and IAV to onset changes.

### 2.4. Mechanistic Analysis of Annual Cycle Changes Using a Simplified Surface Energy Balance Model

To explore how GHG and AER forcings modulate the phase and amplitude of the annual surface temperature cycle, we employ a simplified surface energy balance model. This approach provides a physically grounded framework for diagnosing thermodynamic controls on seasonal variability and has been widely applied in previous studies (Dwyer et al., 2012; Hahn et al., 2022).

The model is governed by the following equation:

$$C \frac{dT}{dt} = Q(t) - \beta T \quad (3)$$

where  $C$  denotes the effective heat capacity of the surface–atmosphere system,  $T$  is the near-surface air temperature,  $Q(t)$  is the net surface energy input independent of temperature (such as net shortwave radiation), and  $\beta$  is a linear damping coefficient that encapsulates the net energy loss.

Applying Fourier analysis to isolate the annual harmonic yields analytical expressions for the phase lag between temperature and energy input,  $= \phi_T - \phi_Q$ , and for amplitude response of temperature to forcing:

$$\phi = \arctan\left(\frac{\nu C}{\beta}\right) \quad (4)$$

$$|T| = \frac{|Q|}{\sqrt{\beta^2 + (\nu C)^2}} \quad (5)$$

where  $\phi_Q$  is calculated from the AC of net radiation,  $\nu = 2\pi \text{ yr}^{-1}$  is the annual angular frequency.  $C$  denotes the effective heat capacity and  $\beta$  represents the bulk damping. These expressions indicate that both the phase and amplitude of the annual temperature cycle are jointly controlled by  $C$  and  $\beta$ .

We estimate  $C$  and damping using a simplified surface energy balance framework.  $C$  represents the thermal inertia of the surface–atmosphere system and is estimated independently of annual-cycle phase by fitting a linearized time-domain energy balance to climatological annual-cycle anomalies. Following F. Song et al. (2020), the effective damping is decomposed into top-of-atmosphere radiative damping  $B$ , diagnosed from regressions of outgoing longwave radiation onto temperature anomalies, and surface–near-surface non-shortwave damping  $\lambda$ , diagnosed from regressions of turbulent non-shortwave flux anomalies onto surface–air temperature difference anomalies. In combination,  $B$  and  $\lambda$  describe the radiative and turbulent contributions to the bulk effective damping relevant to Equation 4. Full details are provided in Text S1 in Supporting Information S1.

### 3. Results

#### 3.1. Observed Contributions of the Annual Cycle and Long-Term Warming to Changes in Summer Onset

We first examine the climatological mean and spatial patterns of seasonal onset across NH midlatitudes during 1950–2014 using daily mean temperatures from the BEST data set (Figure S1 in Supporting Information S1). Summer onset occurs earlier over inland than along coasts, whereas winter onset is delayed inland, particularly over North America (Figure S2 in Supporting Information S1).

Linear trend analyses reveal widespread advances in spring and summer onset over the NH midlatitudes during 1950–2014 (Figure S3 in Supporting Information S1), consistent with previous studies (B.-J. Park et al., 2018; J. Wang et al., 2021), but with pronounced latitudinal and regional heterogeneity. The advances in summer onset weaken poleward, from about 2 days per decade at 30°N to less than 1 day per decade at 60°N (Figure 1a). Strong advances are most evident over Europe, while North America and northern Asia exhibit more modest shifts. These spatial features are robust across ERA5 and Berkeley Earth data sets (Figures S3 and S4 in Supporting Information S1).

To illustrate how idealized changes in the seasonal temperature cycle relate to summer onset timing, Figure S5 in Supporting Information S1 presents a conceptual schematic showing the effects of mean-state shifts, amplitude changes, and phase shifts. In this schematic, uniform warming elevates the entire annual temperature cycle, whereas enhanced amplitude and phase advance represent changes in seasonal contrast and the timing of the cycle, respectively. Guided by this physical framework, we apply a decomposition of Deng et al. (2023) to quantify the contributions of the AC and long-term trend (Figure S6 in Supporting Information S1). The long-term warming contribution largely matches the total summer onset trend in sign and magnitude (Figures 1a and 1b), but its relatively homogeneous pattern cannot explain the observed latitudinal and regional contrasts. For example, in western North America, the observed trend shows only a weak advance in summer onset, whereas the long-term warming component indicates a pronounced advance. Similarly, in Northeast and Northwest Asia, the observed trends form a dipole pattern with weaker advances in the east and stronger advances in the west, while the long-term warming component exhibits the opposite structure. Moreover, the zonal-mean trend of the long-term warming contribution shows little latitudinal variation, averaging about 1.5 days per decade between 30°N and 60°N (Figures 1a and 1b).

This discrepancy highlights the role of changes in the AC. The annual-cycle contribution to summer onset trends (Figure 1c) offsets the warming-driven advance over North America and northern Asia. Although long-term warming advances summer onset by about 1.5 days per decade in both regions, concurrent annual-cycle changes delay onset by 0.57 days per decade in North America and 0.29 days per decade in northern Asia, resulting in only modest net advances. Zonal-mean results further show that annual-cycle-induced delays increase

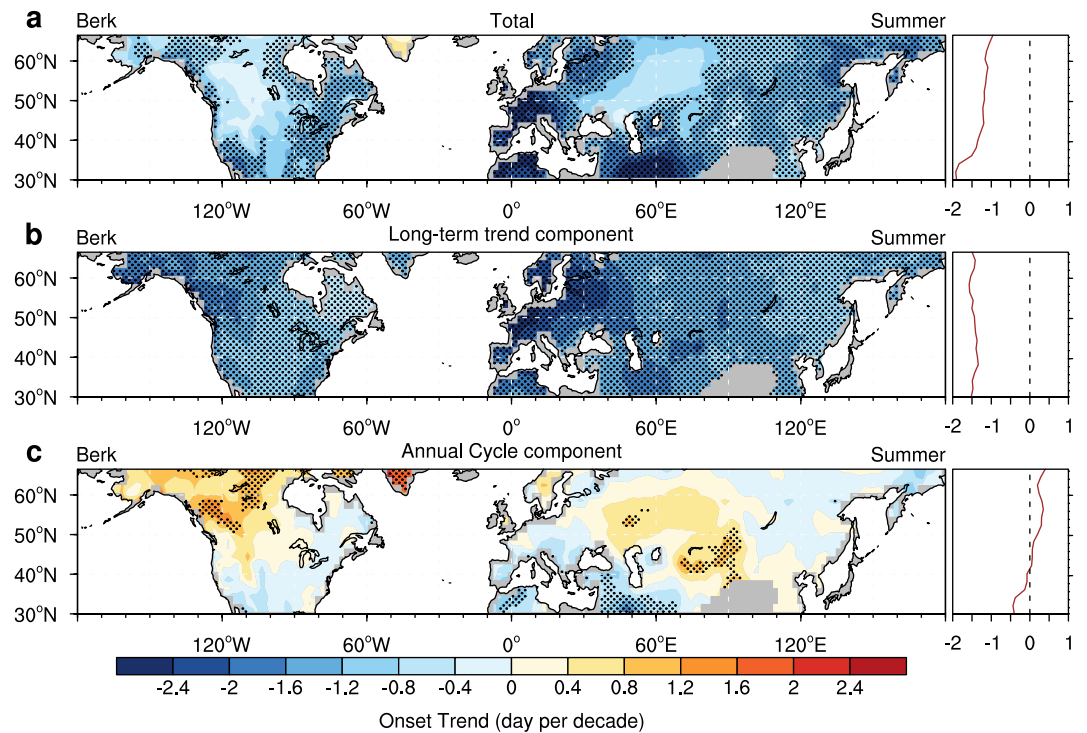


**Figure 1.** Trends in summer onsets during 1950–2014. (a–c) Spatial patterns of linear trends in (a) total summer onset, (b) the long-term trend component, and (c) the annual cycle component. Zonal-mean trends are shown to the right of each panel. Stippling denotes regions with trends significant at the 5% level based on the Mann–Kendall test.

poleward of 40°N, partially compensating for the warming signal and producing the observed spatial heterogeneity. Thus, across NH midlatitudes, particularly over North America and central Asia, seasonal onset changes reflect substantial modulation by the AC in addition to long-term warming. Similar interactions are found for other seasons (Figures S7 and S8 in Supporting Information S1), and the results are robust across ERA5 and Berkeley Earth data sets (Figures S9 and S10 in Supporting Information S1).

### 3.2. Mechanisms Underlying Seasonal Onset Shifts: Role of Annual Cycle Phase Changes

To further understand the drivers of spatial contrasts in AC contributions, we examine the mechanisms governing changes in the phase of the annual temperature cycle using a simplified surface energy balance framework. Within this framework, the effective heat capacity  $C$  represents the thermal inertia of the surface–atmosphere system, whereas the damping is represented by top-of-atmosphere radiative damping  $B$  and surface–near-surface non-shortwave damping  $\lambda$ .

Figure 2 shows spatial patterns of changes in  $C$ ,  $B$ , and  $\lambda$  between 1951–1980 and 1985–2014. Pronounced increases in  $C$  occur over western North America and northern Asia, coinciding with regions of substantial phase delays in the annual temperature cycle, whereas  $C$  tends to be lower over Europe, consistent with the observed phase advance there. These patterns highlight the role of thermal inertia in shaping annual-cycle phase changes. A reduction in  $C$  weakens thermal inertia, allowing surface temperature to respond more rapidly to seasonal forcing and thereby advancing the annual-cycle phase, whereas an increase in  $C$  enhances thermal inertia and delays the phase, leading to a later summer onset. The uneven distribution of changes in historical  $C$  can be understood through region-specific land–atmosphere coupling processes. Specifically, the decline in heat capacity in Europe may be related to enhanced soil moisture drying processes (Y.-N. Wang et al., 2024; Wouters et al., 2022), while the increase in  $C$  in western North America and northern Asia may be associated with intensified permafrost degradation (Varnajot & Makopoulou, 2025) and increased liquid water content during the snowmelt period (Stigter et al., 2021). Phase-based inverse estimates (Figure S13 in Supporting Information S1) and an independent estimate following S. E. Schwartz (2007), in which  $C$  is defined as the ratio of the moist static energy

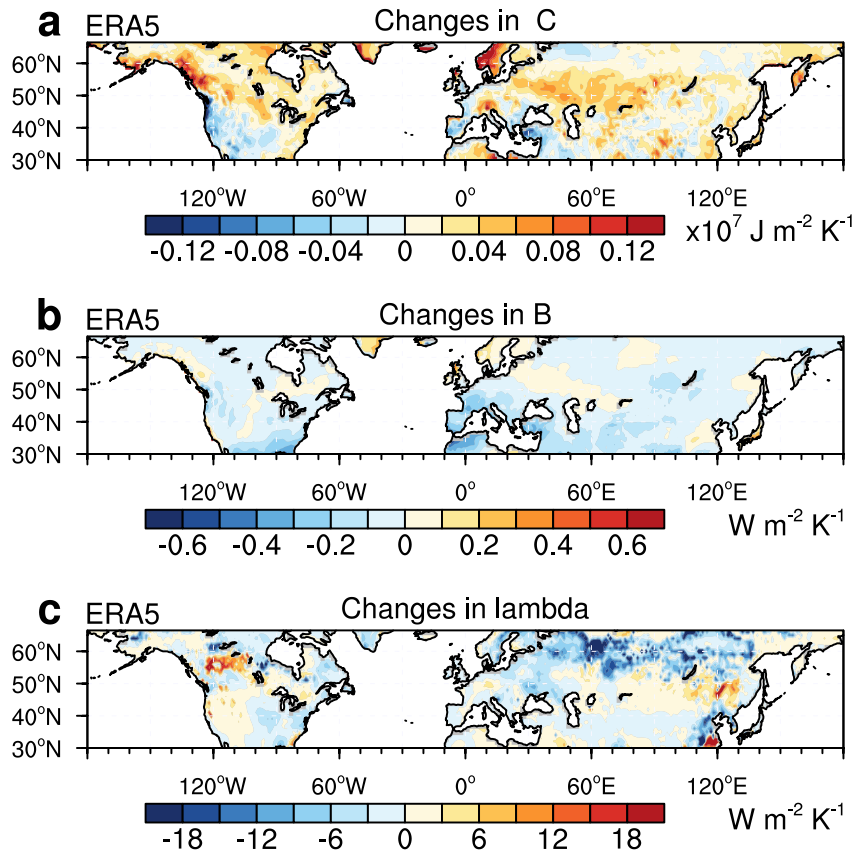


**Figure 2.** Physical processes for changes in annual cycle component diagnosed from ERA5. Changes during 1985–2014 relative to 1951–1980 in (a) effective heat capacity  $C$ , (b) top-of-atmosphere radiative damping  $B$ , and (c) surface–near-surface non-shortwave damping  $\lambda$ .

tendency to the air-temperature tendency (Figure S14 in Supporting Information S1), yield broadly consistent large-scale changes in  $C$ .

Changes in  $B$  and  $\lambda$  are comparatively weak and spatially heterogeneous.  $B$  exhibits a modest overall reduction (Figure 2b), while  $\lambda$  displays mixed-sign patterns that vary across regions (Figure 2c). These damping-related changes do not project coherently onto the large-scale spatial pattern of annual-cycle phase shifts. Instead, the spatial structure of phase changes is more closely aligned with variations in  $C$ , underscoring the dominant role of thermal inertia in shaping the observed regional contrasts.

### 3.3. Anthropogenic Forcings and Physical Mechanisms Driving Changes in the Annual Cycle

Given the critical role of the AC in modulating seasonal onset, we use CMIP6 ALL-forcing and single-forcing experiments to assess the influence of external forcings on trends in the annual-cycle component.

A Taylor diagram analysis shows that nine selected models reproduce the climatological onset distribution well (Figure S15 in Supporting Information S1). Under ALL forcing, the multimodel ensemble captures the observed spatial patterns of AC trends, including pronounced summer AC anomalies over western North America and northern Asia (Figure 3a), although the simulated amplitude is weaker than observed.

Attribution results reveal distinct regional patterns in the relative contributions of different anthropogenic forcings. Single-forcing experiments further clarify the respective roles of GHG and AER. Over western North America and northern Asia, GHG-forcing simulations exhibit AC-related summer onset trends of opposite sign to observations (Figure 3b). In contrast, AER-forcing tends to induce summer onset delays associated with AC changes that are broadly consistent in sign with the ALL-forcing response (Figure 3c), although the inter-model agreement is relatively weaker. Notably, under AER-forcing, central Europe and England exhibit an earlier

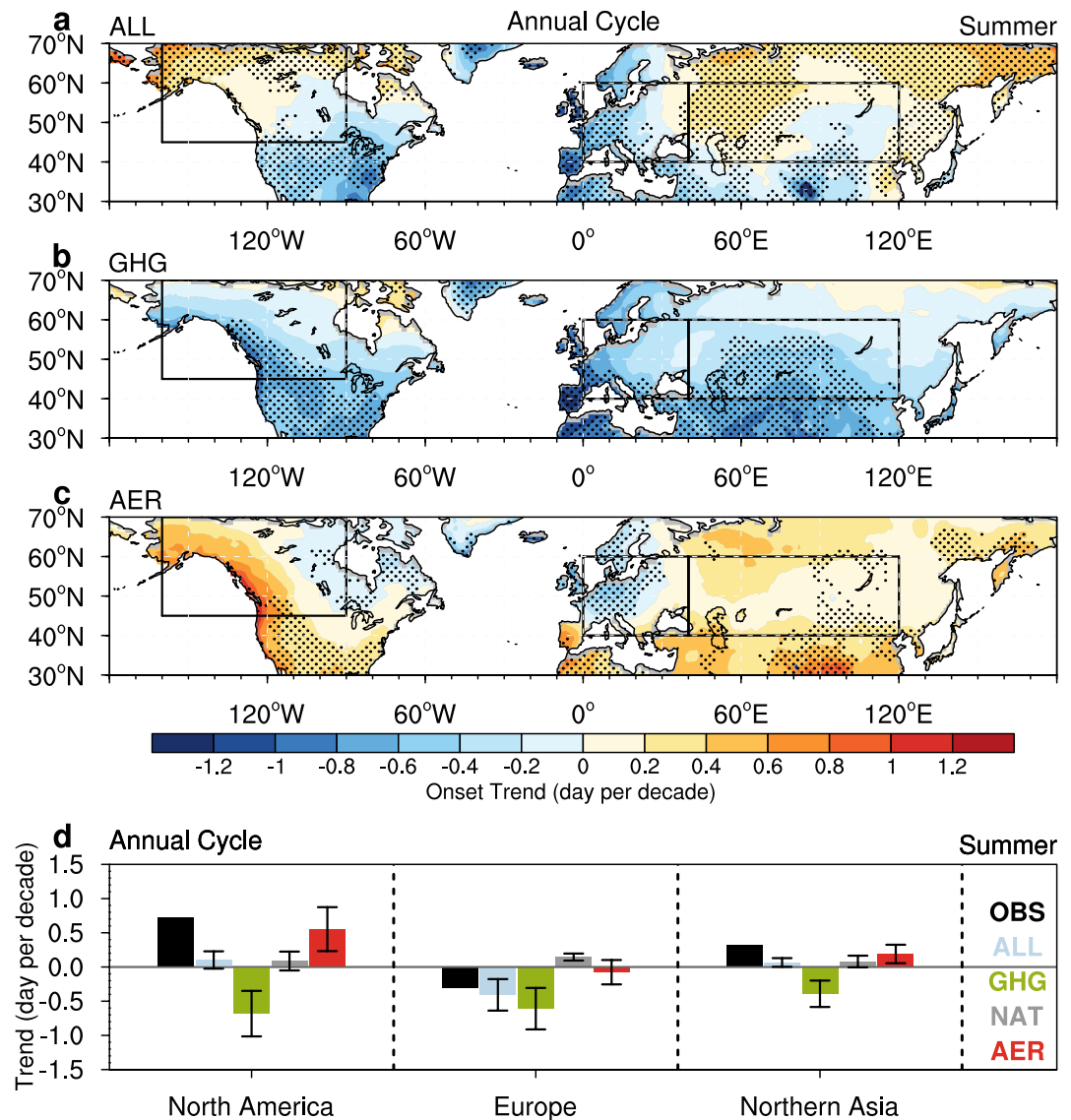


**Figure 3.** Anthropogenic influences on summer onset changes. (a–c) Trends in annual cycle (AC) component under (a) ALL, (b) greenhouse gas, and (c) AER forcing. Shading represents the multimodel ensemble mean trends; dots indicate regions where 6 out of 9 models agree on the sign of change. (d) Regional-mean trends in the AC component of summer onset (1950–2014) over North America (45°N–70°N, 160°W–90°W), Europe (40°N–60°N, 0°E–40°E), and northern Asia (40°N–60°N, 40°E–120°E) from CMIP6 simulations under four forcings. Error bars denote 1 standard deviation from 10,000 bootstrap resamples.

summer onset, aligning with the influence of GHG-forcing and contrasting with the response observed in most other NH regions. Consistent with the spatial patterns, the regional-mean trends highlight the opposing influences of AER and GHG on AC-related summer onset changes over North America and northern Asia (Figure 3d). By contrast, over Europe, both GHG and AER forcings contribute to AC-related summer onset changes with the same sign, consistent with the regional-mean estimates shown in Figure 3d.

Given the contrasting AC-phase responses to GHG and AER forcing, we diagnose the mechanisms using a simplified surface energy-balance framework. Using CMIP6 single-forcing simulations, we quantify changes in  $C$ ,  $B$ , and  $\lambda$  between 1951–1980 and 1985–2014 and assess their contributions to seasonal-onset shifts (Figure 4).

According to Equation 4, the phase of the annual temperature cycle is governed by the ratio of effective thermal inertia to effective damping ( $\nu C/\beta$ ). Thus, a decrease in  $C$  and/or an increase in damping (through  $B$  and  $\lambda$ ) reduces

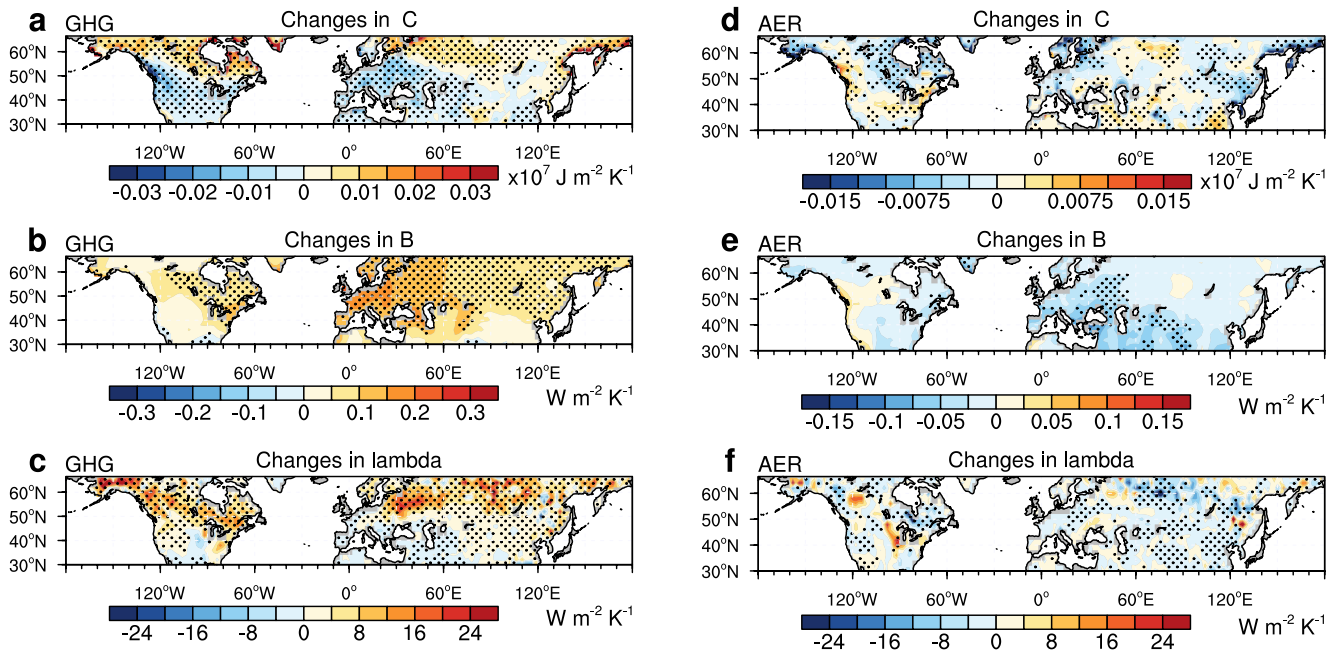


**Figure 4.** Thermal response changes under greenhouse gas (GHG) and AER forcing. (a–c) Changes in (a) effective heat capacity  $C$ , (b) top-of-atmosphere radiative damping  $B$ , and (c) surface–near-surface non-shortwave damping  $\lambda$  for 1985–2014 relative to 1951–1980 in CMIP6 GHG-only simulations. (d–f) As in (a–c), but for AER forcing. Stippling indicates regions where at least 6 of 9 models agree on the sign.

$\nu C/\beta$  and advances the timing of the annual temperature maximum, whereas the opposite changes delay it. Under GHG-forcing, changes in  $C$  and damping are consistent with Dwyer et al. (2012). At high latitudes, GHG-induced sea ice loss enhances the role of the ocean mixed layer, increasing  $C$ , whereas soil drying at mid-to-low latitudes reduces thermal inertia, leading to a slight decrease in  $C$ . Summer onset advances across North America, Europe, and northern Asia (Figure 3b), accompanied by pronounced reductions in  $C$  (Figure 4a), indicating weakened thermal inertia and a faster seasonal temperature adjustment, with a corresponding phase advance. Concurrently, the  $B$  increases over large parts of the NH (Figure 4b), consistent with enhanced outgoing longwave radiation under warming, which further contributes to phase advancement through strengthened effective damping. Changes in  $\lambda$  are more heterogeneous, but positive anomalies over North America and northern Asia (Figure 4c) further support phase advancement in these regions.

In contrast, AER-forcing delays summer onset over North America and northern Asia (Figure 3c), together with slight increases in  $C$  (Figure 4d) and a broad reduction in  $B$  (Figure 4e), consistent with weaker radiative damping and a delayed phase. Changes in  $\lambda$  are spatially heterogeneous, but negative anomalies over parts of northern Asia (Figure 4f) imply reduced damping there. Aerosol-induced surface cooling suppresses evaporation and slows soil moisture depletion, increasing  $C$  (Yu et al., 2002), whereas reduced surface shortwave radiation weakens turbulence and boundary-layer mixing, reducing damping (Persad et al., 2017). Notably, over Europe and North America after the 1980s, declining aerosol emissions tend to enhance surface warming, suggesting that the diagnosed damping response represents an effective dynamical and radiative adjustment under aerosol forcing, rather than a direct cooling effect. Nevertheless, the changes in damping are consistent with the delayed phase of the annual temperature cycle under aerosol forcing. As shown by Dwyer et al. (2012), low-latitude phase changes are primarily controlled by damping: stronger damping under GHG advances the peak, whereas weaker damping under AER delays it. A complementary phase-based estimate further supports the inferred changes in  $C$  (Figure S16 in Supporting Information S1).

#### 4. Conclusions

This study investigates changes in seasonal onset across NH midlatitudes from 1950 to 2014, with a focus on the role of the AC. By decomposing the seasonal temperature signal, we demonstrate that AC variations exert a critical influence on summer onset. Importantly, their effects often counteract long-term warming, substantially

offsetting the trend toward earlier summers in key midlatitude regions such as North America, Europe, and northern Asia.

Using a simplified surface energy balance framework, we show that variations in  $C$ , together with changes in effective damping, play a central role in controlling the phase of the AC. Regional contrasts, such as advances over Europe and delays over northern Asia, are primarily associated with differences in effective heat capacity. In western North America, the changes are associated with increased  $C$ , while changes in damping are comparatively weaker and spatially less coherent.

Using CMIP6 single-forcing simulations, we disentangle the anthropogenic drivers of these AC changes. The results reveal that aerosol forcing induces delayed summer onset over western North America and parts of northern Asia, accompanied by increases in  $C$  and a weakening of radiative damping. In contrast, GHG forcing reduces  $C$  and enhances damping, jointly advancing seasonal transitions, particularly over midlatitude continental regions.

While we decompose seasonal-onset changes into contributions from long-term mean warming and temperature annual-cycle variations, these two components need not be fully independent in the climate system. Long-term warming can alter boundary conditions, including sea ice, snow cover, and soil moisture, reshaping the seasonal structure of the surface energy balance and thereby modifying the amplitude and phase of the temperature AC (e.g., Stine et al., 2009). This coupling implies that the annual-cycle component isolated here may already include part of the forced warming response. Future work using longer observational records and targeted sensitivity experiments with idealized climate models could help constrain the mechanisms and quantify the importance of these interactions.

### Conflict of Interest

The authors declare no conflicts of interest relevant to this study.

### Data Availability Statement

The CMIP6 data are available online at <https://esgf-node.llnl.gov/projects/cmip6/>. ERA5 reanalysis data (Hersbach et al., 2023) are provided by the Copernicus Climate Change Service (C3S). The Berkeley Earth Surface Temperature data set (Rohde & Hausfather, 2020) is available from the Berkeley Earth website (<https://berkeleyearth.org/data/>). All data sets were last accessed on 15 September 2024. The CMIP6 models used in this study are listed in Table S1 in Supporting Information S1.

### Acknowledgments

The work was supported by the National Natural Science Foundation of China (Grants 42406006, 42530606, 42261144687, and 42405031).

### References

- Anenberg, S. C., Weinberger, K. R., Roman, H., Neumann, J. E., Crimmins, A., Fann, N., et al. (2017). Impacts of oak pollen on allergic asthma in the United States and potential influence of future climate change. *GeoHealth*, 1(3), 80–92. <https://doi.org/10.1002/2017GH000055>
- Both, C., Bouwhuis, S., Lessells, C., & Visser, M. E. (2006). Climate change and population declines in a long-distance migratory bird. *Nature*, 441(7089), 81–83. <https://doi.org/10.1038/nature04539>
- Buermann, W., Forkel, M., O'sullivan, M., Sitch, S., Friedlingstein, P., Haverd, V., et al. (2018). Widespread seasonal compensation effects of spring warming on northern plant productivity. *Nature*, 562(7725), 110–114. <https://doi.org/10.1038/s41586-018-0555-7>
- Chiang, J. C. H., Atwood, A. R., Vimont, D. J., Nicknisch, P. A., Roberts, W. H. G., Tabor, C. R., & Broccoli, A. J. (2022). Two annual cycles of the Pacific cold tongue under orbital precession. *Nature*, 611(7935), 295–300. <https://doi.org/10.1038/s41586-022-05240-9>
- Christidis, N., Stott, P. A., Brown, S., Karoly, D. J., & Caesar, J. (2007). Human contribution to the lengthening of the growing season during 1950–99. *Journal of Climate*, 20(21), 5441–5454. <https://doi.org/10.1175/2007JCLI1568.1>
- Cleland, E. E., Chuine, I., Menzel, A., Mooney, H. A., & Schwartz, M. D. (2007). Shifting plant phenology in response to global change. *Trends in Ecology & Evolution*, 22(7), 357–365. <https://doi.org/10.1016/j.tree.2007.04.003>
- Deng, Q., Wang, Y., Tan, X., & Fu, Z. (2023). The role of semiannual cycle in modulating seasonality changes of surface air temperature over China and its mechanism. *Climate Dynamics*, 61(7), 3353–3365. <https://doi.org/10.1007/s00382-023-06748-0>
- Donohue, A., Dawson, E., McMurdie, L., Battisti, D. S., & Rhines, A. (2020). Seasonal asymmetries in the lag between insolation and surface temperature. *Journal of Climate*, 33(10), 3921–3945. <https://doi.org/10.1175/JCLI-D-19-0329.1>
- Duan, J., Ma, Z., Wu, P., Xoplaki, E., Hegerl, G., Li, L., et al. (2019). Detection of human influences on temperature seasonality from the nineteenth century. *Nature Sustainability*, 2(6), 484–490. <https://doi.org/10.1038/s41893-019-0276-4>
- Dwyer, J. G., Biasutti, M., & Sobel, A. H. (2012). Projected changes in the seasonal cycle of surface temperature. *Journal of Climate*, 25(18), 6359–6374. <https://doi.org/10.1175/JCLI-D-11-00741.1>
- García-Herrera, R., Díaz, J., Trigo, R. M., Luterbacher, J., & Fischer, E. M. (2010). A review of the European summer heat wave of 2003. *Critical Reviews in Environmental Science and Technology*, 40(4), 267–306. <https://doi.org/10.1080/10643380802238137>
- Gillett, N. P., Shiogama, H., Funke, B., Hegerl, G., Knutti, R., Matthes, K., et al. (2016). The detection and attribution model intercomparison project (DAMIP v1. 0) contribution to CMIP6. *Geoscientific Model Development*, 9(10), 3685–3697. <https://doi.org/10.5194/gmd-9-3685-2016>

- Hahn, L. C., Armour, K. C., Battisti, D. S., Eisenman, I., & Bitz, C. M. (2022). Seasonality in Arctic warming driven by sea ice effective heat capacity. *Journal of Climate*, *35*(5), 1629–1642. <https://doi.org/10.1175/JCLI-D-21-0626.1>
- Hersbach, H., Bell, B., Berrisford, P., Biavati, G., Horányi, A., Muñoz Sabater, J., et al. (2023). ERA5 hourly data on single levels from 1940 to present. *Copernicus Climate Change Service (C3S) Climate Data Store (CDS)*. <https://doi.org/10.24381/cds.adbb2d47>
- Hersbach, H., Bell, B., Berrisford, P., Hirahara, S., Horányi, A., Muñoz-Sabater, J., et al. (2020). The ERA5 global reanalysis. *Quarterly Journal of the Royal Meteorological Society*, *146*(730), 1999–2049. <https://doi.org/10.1002/qj.3803>
- Horton, K. G., La Sorte, F. A., Sheldon, D., Lin, T.-Y., Winner, K., Bernstein, G., et al. (2020). Phenology of nocturnal Avian migration has shifted at the continental scale. *Nature Climate Change*, *10*(1), 63–68. <https://doi.org/10.1038/s41558-019-0648-9>
- Jo, A. R., Lee, J. Y., Timmermann, A., Jin, F. F., Yamaguchi, R., & Gallego, A. (2022). Future amplification of sea surface temperature seasonality due to enhanced ocean stratification. *Geophysical Research Letters*, *49*(9), e2022GL098607. <https://doi.org/10.1029/2022GL098607>
- Keeling, C. D., Chin, J., & Whorf, T. (1996). Increased activity of northern vegetation inferred from atmospheric CO<sub>2</sub> measurements. *Nature*, *382*(6587), 146–149. <https://doi.org/10.1038/382146a0>
- Lin, W., & Wang, C. (2023). Detection and attribution of the summer length changes in the Northern Hemisphere. *Climate Dynamics*, *60*(11), 3801–3812. <https://doi.org/10.1007/s00382-022-06553-1>
- Liu, F., Lu, J., Luo, Y., Huang, Y., & Song, F. (2020). On the Oceanic origin for the enhanced seasonal cycle of SST in the midlatitudes under global warming. *Journal of Climate*, *33*(19), 8401–8413. <https://doi.org/10.1175/JCLI-D-20-0114.1>
- Liu, F., Song, F., & Luo, Y. (2024). Human-induced intensified seasonal cycle of sea surface temperature. *Nature Communications*, *15*(1), 3948. <https://doi.org/10.1038/s41467-024-48381-3>
- Lv, S., Song, F., Dong, H., & Wu, L. (2024). Phase and amplitude changes in rainfall annual cycle over global land monsoon regions under global warming. *Geophysical Research Letters*, *51*(12), e2024GL108496. <https://doi.org/10.1029/2024GL108496>
- Matiu, M., Ankerst, D. P., & Menzel, A. (2017). Interactions between temperature and drought in global and regional crop yield variability during 1961–2014. *PLoS One*, *12*(5), e0178339. <https://doi.org/10.1371/journal.pone.0178339>
- Menzel, A. (2000). Trends in phenological phases in Europe between 1951 and 1996. *International Journal of Biometeorology*, *44*(2), 76–81. <https://doi.org/10.1007/s004840000054>
- Paluš, M., Novotná, D., & Tichavský, P. (2005). Shifts of seasons at the European mid-latitudes: Natural fluctuations correlated with the North Atlantic Oscillation. *Geophysical Research Letters*, *32*(12), L12805. <https://doi.org/10.1029/2005GL022838>
- Park, B.-J., Kim, Y.-H., Min, S.-K., & Lim, E.-P. (2018). Anthropogenic and natural contributions to the lengthening of the summer season in the Northern Hemisphere. *Journal of Climate*, *31*(17), 6803–6819. <https://doi.org/10.1175/JCLI-D-17-0643.1>
- Park, T., Ganguly, S., Tømmervik, H., Euskirchen, E. S., Høgda, K.-A., Karlsen, S. R., et al. (2016). Changes in growing season duration and productivity of northern vegetation inferred from long-term remote sensing data. *Environmental Research Letters*, *11*(8), 084001. <https://doi.org/10.1088/1748-9326/11/8/084001>
- Peña-Ortiz, C., Barriopedro, D., & García-Herrera, R. (2015). Multidecadal variability of the summer length in Europe. *Journal of Climate*, *28*(13), 5375–5388. <https://doi.org/10.1175/JCLI-D-14-00429.1>
- Persad, G. G., Paynter, D. J., Ming, Y., & Ramaswamy, V. (2017). Competing atmospheric and surface-driven impacts of absorbing aerosols on the East Asian summertime climate. *Journal of Climate*, *30*(22), 8929–8949. <https://doi.org/10.1175/JCLI-D-16-0860.1>
- Qian, C., Fu, C., Wu, Z., & Yan, Z. (2011). The role of changes in the annual cycle in earlier onset of climatic spring in northern China. *Advances in Atmospheric Sciences*, *28*(2), 284–296. <https://doi.org/10.1007/s00376-010-9221-1>
- Qian, C., & Zhang, X. (2015). Human influences on changes in the temperature seasonality in mid- to high-latitude land areas. *Journal of Climate*, *28*(15), 5908–5921. <https://doi.org/10.1175/JCLI-D-14-00821.1>
- Reyes-Fox, M., Steltzer, H., Trlica, M., McMaster, G. S., Andales, A. A., LeCain, D. R., & Morgan, J. A. (2014). Elevated CO<sub>2</sub> further lengthens growing season under warming conditions. *Nature*, *510*(7504), 259–262. <https://doi.org/10.1038/nature13207>
- Rohde, R. A., & Hausfather, Z. (2020). The Berkeley Earth land/ocean temperature record. *Earth System Science Data*, *12*(4), 3469–3479. <https://doi.org/10.5194/essd-12-3469-2020>
- Ryan, S. J., Carlson, C. J., Mordecai, E. A., & Johnson, L. R. (2019). Global expansion and redistribution of Aedes-borne virus transmission risk with climate change. *PLoS Neglected Tropical Diseases*, *13*(3), e0007213. <https://doi.org/10.1371/journal.pntd.0007213>
- Santer, B. D., Po-Chedley, S., Feldl, N., Fyfe, J. C., Fu, Q., Solomon, S., et al. (2022). Robust anthropogenic signal identified in the seasonal cycle of tropospheric temperature. *Journal of Climate*, *35*(18), 6075–6100. <https://doi.org/10.1175/JCLI-D-21-0766.1>
- Santer, B. D., Po-Chedley, S., Zelinka, M. D., Cvijanovic, I., Bonfils, C., Durack, P. J., et al. (2018). Human influence on the seasonal cycle of tropospheric temperature. *Science*, *361*(6399), eaas8806. <https://doi.org/10.1126/science.aas8806>
- Schwartz, M. D., Ahas, R., & Aasa, A. (2006). Onset of spring starting earlier across the Northern Hemisphere. *Global Change Biology*, *12*(2), 343–351. <https://doi.org/10.1111/j.1365-2486.2005.01097.x>
- Schwartz, S. E. (2007). Heat capacity, time constant, and sensitivity of Earth's climate system. *Journal of Geophysical Research*, *112*(D24), D24S05. <https://doi.org/10.1029/2007JD008746>
- Shi, J.-R., Santer, B. D., Kwon, Y.-O., & Wijffels, S. E. (2024). The emerging human influence on the seasonal cycle of sea surface temperature. *Nature Climate Change*, *14*(4), 364–372. <https://doi.org/10.1038/s41558-024-01958-8>
- Song, F., Leung, L. R., Lu, J., Zhou, T., & Huang, P. (2023). Advances in understanding the changes of tropical rainfall annual cycle: A review. *Environmental Research: Climate*, *2*(4), 042001. <https://doi.org/10.1088/2752-5295/acf606>
- Song, F., Lu, J., Leung, L. R., & Liu, F. (2020). Contrasting phase changes of precipitation annual cycle between land and ocean under global warming. *Geophysical Research Letters*, *47*(20), e2020GL090327. <https://doi.org/10.1029/2020GL090327>
- Sparks, T. H., & Menzel, A. (2002). Observed changes in seasons: An overview. *International Journal of Climatology: A Journal of the Royal Meteorological Society*, *22*(14), 1715–1725. <https://doi.org/10.1002/joc.821>
- Steltzer, H., & Post, E. (2009). Seasons and life cycles. *Science*, *324*(5929), 886–887. <https://doi.org/10.1126/science.1171542>
- Stigter, E. E., Steiner, J. F., Koch, I., Saloranta, T. M., Kirkham, J. D., & Immerzeel, W. W. (2021). Energy and mass balance dynamics of the seasonal snowpack at two high-altitude sites in the Himalaya. *Cold Regions Science and Technology*, *183*, 103233. <https://doi.org/10.1016/j.coldregions.2021.103233>
- Stine, A. R., Huybers, P., & Fung, I. Y. (2009). Changes in the phase of the annual cycle of surface temperature. *Nature*, *457*(7228), 435–440. <https://doi.org/10.1038/nature07675>
- Timmermann, A., Jin, F. F., & Collins, M. (2004). Intensification of the annual cycle in the tropical Pacific due to greenhouse warming. *Geophysical Research Letters*, *31*(12), L12208. <https://doi.org/10.1029/2004GL019442>
- Varnajot, A., & Makopoulou, E. (2025). Tourism in the Arctic is at risk due to intensifying permafrost degradation. *Communications Earth & Environment*, *6*(1), 983. <https://doi.org/10.1038/s43247-025-02944-4>

- Wang, J., Guan, Y., Wu, L., Guan, X., Cai, W., Huang, J., et al. (2021). Changing lengths of the four seasons by global warming. *Geophysical Research Letters*, *48*(6), e2020GL091753. <https://doi.org/10.1029/2020GL091753>
- Wang, Y.-N., Zuo, Z.-Y., Qiao, L., Zhang, K.-W., Chang, M.-Y., Xiao, D., et al. (2024). Amplification effect of intra-seasonal variability of soil moisture on heat extremes over Eurasia. *Advances in Climate Change Research*, *15*(1), 1–8. <https://doi.org/10.1016/j.accre.2024.01.008>
- Wouters, H., Keune, J., Petrova, I. Y., Van Heerwaarden, C. C., Teuling, A. J., Pal, J. S., et al. (2022). Soil drought can mitigate deadly heat stress thanks to a reduction of air humidity. *Science Advances*, *8*(1), eabe6653. <https://doi.org/10.1126/sciadv.abe6653>
- Wu, Z., Schneider, E. K., Kirtman, B. P., Sarachik, E. S., Huang, N. E., & Tucker, C. J. (2008). The modulated annual cycle: An alternative reference frame for climate anomalies. *Climate Dynamics*, *31*(7), 823–841. <https://doi.org/10.1007/s00382-008-0437-z>
- Yang, F., Chiang, J. C. H., & Wu, Z. (2025). What causes the hemispheric difference in the asymmetry of the temperature annual cycle? *Geophysical Research Letters*, *52*(7), e2024GL112611. <https://doi.org/10.1029/2024GL112611>
- Yang, F., & Wu, Z. (2024). The phase change in the annual cycle of sea surface temperature. *npj Climate and Atmospheric Science*, *7*(1), 48. <https://doi.org/10.1038/s41612-024-00591-8>
- Yu, H., Liu, S., & Dickinson, R. (2002). Radiative effects of aerosols on the evolution of the atmospheric boundary layer. *Journal of Geophysical Research*, *107*(D12), AAC3-1–AAC3-14. <https://doi.org/10.1029/2001JD000754>